Influence of Light-Induced Conical Intersection on the Photodissociation Dynamics of D-2(+) Starting from Individual Vibrational Levels

ARTICLE *in* THE JOURNAL OF PHYSICAL CHEMISTRY A · JUNE 2014

Impact Factor: 2.69 · DOI: 10.1021/jp504889e · Source: PubMed

4 AUTHORS, INCLUDING:

András Csehi
University of Debrecen
13 PUBLICATIONS **27** CITATIONS
SEE PROFILE

Ágnes vibók
University of Debrecen
103 PUBLICATIONS **1,116** CITATIONS
SEE PROFILE

THE JOURNAL OF PHYSICAL CHEMISTRY A

Article

pubs.acs.org/JPCA

Influence of Light-Induced Conical Intersection on the Photodissociation Dynamics of D_2^+ Starting from Individual Vibrational Levels

Gábor J. Halász,[†] András Csehi,[‡] Ágnes Vibók,*[,‡] and Lorenz S. Cederbaum[§]

[†]Department of Information Technology, University of Debrecen, P.O. Box 12, H-4010 Debrecen, Hungary

[‡]Department of Theoretical Physics, University of Debrecen, P.O. Box 5, H-4010 Debrecen, Hungary

[§]Theoretische Chemie, Physikalish-Chemisches Institut, Universität Heidelberg, H-69120 Heidelberg, Germany

ABSTRACT: Previous works have shown that dressing of diatomic molecules by standing or by running laser waves gives rise to the appearance of so-called light-induced conical intersections (LICIs). Because of the strong nonadiabatic couplings, the existence of such LICIs may significantly change the dynamical properties of a molecular system. In our former paper (*J. Phys. Chem. A* **2013**, *117*, 8528), the photodissociation dynamics of the D_2^+ molecule were studied in the LICI framework starting the initial vibrational nuclear wave packet from the superposition of all the vibrational states initially produced by ionizing D_2. The present work complements our previous investigation by letting the initial nuclear wave packets start from different individual vibrational levels of D_2^+, in particular, above the energy of the LICI. The kinetic energy release spectra, the total dissociation probabilities, and the angular distributions of the photofragments are calculated and discussed. An interesting phenomenon has been found in the spectra of the photofragments. Applying the light-induced adiabatic picture supported by LICI, explanations are given for the unexpected structure of the spectra.

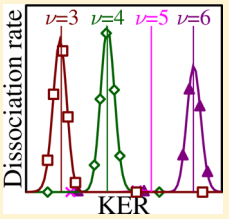

I. INTRODUCTION

This paper addresses the photodissociation dynamics of the D_2^+ molecule via a laser-induced conical intersection (LICI)[1−8] starting the nuclear wave packet from single vibrational eigenstates. To understand the essence of the LICI phenomenon, we should refresh our knowledge about the peculiarities of the so-called "natural conical intersections" (CIs). CI topologies are ubiquitous in molecules, and information on their crucial role in the quantum dynamics of polyatomic systems has been provided by many important studies.[10−16] In the vicinity of CIs, the Born−Oppenheimer adiabatic approximation breaks down: the adiabatic potential energy surfaces become degenerate, giving rise to singularities in the nonadiabatic coupling. In this case, the electronic states are strongly coupled by the nuclear motion, and the energy exchange between the fast electrons and the slow nuclei becomes significant. As a result, CIs act as "photochemical funnels" inducing the ultrafast decay of the initially excited electronic state, typically on a femtosecond time scale.

To form a CI, the molecular system must have at least two independent nuclear degrees of freedom. Therefore, having only one nuclear degree of freedom in a molecule (for example, diatomics), CIs never can appear. However, if an additional degree of freedom associated with the system due to some interaction with an environment (this is the situation, for example, in the case of laser molecule interaction), then CIs can be formed. It was pointed out in previous papers[1,2] that CIs can be created both by running or by standing laser waves even in diatomics. The rotation of the molecules exposed to strong laser fields can serve as an additional degree of freedom because the interaction of the transition dipole moment of the system with the electric field leads to an effective torque toward the polarization direction of the light. In the correct dynamical description, one has to explicitly include this light-matter interaction into the Hamiltonian, and the change of nuclear dynamics due to the external laser field can be considered as arising from the appearance of a "light-induced conical intersection" (LICI). The positions of these light-induced CIs are determined by the laser frequency and the strengths of their nonadiabatic couplings by the intensity of the laser. It has been demonstrated in several former theoretical works that LICIs have strong impact on the dynamical properties of diatomics.[3−9] Motivated by these theoretical predictions on the LICIs in diatomics, a recent experiment[17] on the laser-induced isomerization of a polyatomic molecule was qualitatively interpreted with the help of the concept of LICIs. The additional degrees of freedom in polyatomic molecules add much to the richness of the phenomenon of LICIs and open the door to its exploitation, as has been shown in ref 18.

The dissociation process of the D_2^+ molecule has been extensively studied for more than two decades.[19−44] In our recent work,[7] the impact of the LICI on the photodissociation dynamics of the D_2^+ molecule was discussed starting from the Franck−Condon (FC) distribution of the vibrational states in the initial wave function, as can be achieved by first photoionizing D_2. Full 2D calculations were compared with

Special Issue: David R. Yarkony Festschrift

Received: May 18, 2014
Revised: June 14, 2014

dx.doi.org/10.1021/jp504889e | *J. Phys. Chem. A* XXXX, XXX, XXX−XXX

those obtained from the common 1D model. In the 1D simulations, the molecular rotational angle is only a parameter; that is, the LICI was not included, while in the 2D simulations the rotational angle is considered as a dynamic variable; therefore, the LICI is taken explicitly into account. The obtained 1D and 2D results strongly differ from each other, demonstrating the significant impact of the LICI on the dissociation dynamics of D_2^+.

The purpose of the present work is to investigate the influence of the LICI on the kinetic energy release (KER) spectra and on the angular distributions of the photofragments but starting this time from different individual vibrational eigenstates of D_2^+. Again, we solve the nuclear Schrödinger equation for both the 1D and 2D models. By studying the spectra, an unforeseen phenomenon has been observed. Launching the initial nuclear wave packet from a certain vibrational eigenstate, the dissociation probability can tend to zero. Which of the vibrational levels exhibits this behavior strongly depends on the energy and intensity of the applied laser field. Within the present study, we mainly focus on visualizing and understanding this issue.

The subsequent sections of this paper are organized as follows. In Section II, the evolution of the nuclear wave packet by using the MCTDH method is described. The results on the KER spectra, total photodissociation probabilities, as well as on the angular distributions and their interpretation are presented in Section III. Section IV briefly provides the conclusions and the perspectives.

II. PHYSICAL SITUATION AND METHODS

Our model and numerical method were discussed in detail previously in ref 7. Here only the applied Hamiltonian and a few relevant details of the numerical calculations are briefly summarized. Consider the two energy levels of the D_2^+ ion, which are relevant to the process under investigation: These are the electronic ground (V_1 = $1s\sigma_g$) and the first excited (V_2 = $2p\sigma_u$) eigenstates of the field-free Hamiltonian. Assume further that initially the D_2^+ ion is in its ground electronic ($1s\sigma_g$) as well as in its ground rotational state but is one of its vibrational eigenstates. (See Figure 1.) Let us now excite by a resonant laser pulse the $1s\sigma_g$ ground state of the ion to the repulsive $2p\sigma_u$ state. (See also Figure 1.) Because of this excitation, the laser light induces a radiative coupling between these two electronic states. The respective nonvanishing transition-dipole matrix element is responsible for the light-induced electronic transition. In the space of these two electronic states the total molecule-plus-field Hamiltonian for the rovibronic nuclear motions reads

$$H = \begin{pmatrix} -\frac{1}{2\mu}\frac{\partial^2}{\partial R^2} + \frac{L_{\theta\varphi}^2}{2\mu R^2} & 0 \\ 0 & -\frac{1}{2\mu}\frac{\partial^2}{\partial R^2} + \frac{L_{\theta\varphi}^2}{2\mu R^2} \end{pmatrix} + \begin{pmatrix} V_1(R) & -\epsilon_0 f(t)\, \mathrm{d}(R) \cos\theta \cos\omega_L t \\ -\epsilon_0 f(t)\, \mathrm{d}(R) \cos\theta \cos\omega_L t & V_2(R) \end{pmatrix} \quad (1)$$

Here R and (θ, φ) are the molecular vibrational and rotational coordinates, respectively, μ is the reduced mass, and $L_{\theta\varphi}$ denotes the angular momentum operator of the nuclei. One of the rotational coordinates, θ, denotes the angle between the polarization direction of the laser light and the direction of the transition dipole. $V_1(R)$ ($1s\sigma_g$) and $V_2(R)$ ($2p\sigma_u$) are the energy

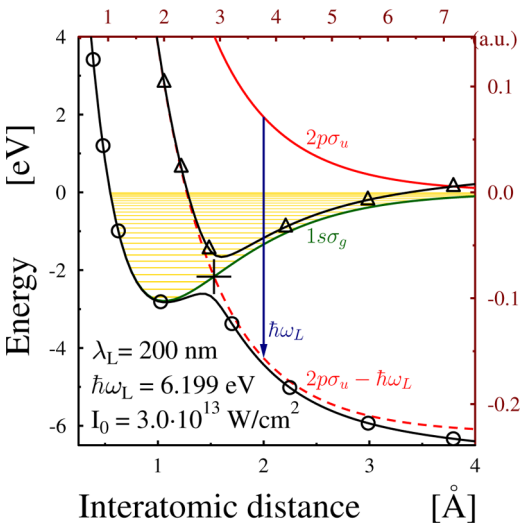

Figure 1. A cut through the potential energy surface of the D_2^+ molecule as a function of interatomic separation. Diabatic energies of the ground ($1s\sigma_g$) and the first excited ($2p\sigma_u$) states are displayed with solid green and red lines, respectively. The field-dressed excited state ($2p\sigma_u - \hbar\omega_L$; dashed red line) forms a light-induced conical intersection (LICI) with the ground state. For the case of a laser frequency ω_L = 6.199 eV and field intensity of 3×10^{13}(W/cm^2), a cut through the adiabatic surfaces at θ = 0 (parallel to the field) is also shown by solid black lines marked with circles (V_{lower}) and triangles (V_{upper}). We denote with a cross the position of the LICI (R_{LICI} = 1.53 Å = 2.891 a.u. and E_{LICI} = −2.16611eV).

curves of the two electronic states coupled by the laser (whose frequency is ω_L and amplitude is ϵ_0), $f(t)$ is the envelop function of the laser pulse, and $d(R)$ ($= -\langle\psi_1^e|\sum_j r_j|\psi_1^e\rangle$) is the transition dipole matrix element ($e = m_e = \hbar$ =1; atomic units are used throughout the article). The potential energies $V_1(R)$ and $V_2(R)$ and the transition dipole moment were taken from refs 45 and 46. Using the dressed state representation picture, we can easily demonstrate the essence of the light-induced nonadiabatic effects. (See refs 3 and 6 for a detailed discussion.) After absorption of one photon, the energy of the ground electronic state is shifted upward or equivalently, and the $2p\sigma_u$ repulsive excited potential curve is shifted downward by $\hbar\omega_L$, and a crossing between the diabatic ground and excited potential energy curves is formed. New light-induced adiabatic states V_{lower} and V_{upper} (Figure 1) are obtained after diagonalizing the diabatic potential energy matrix eq 1. These two surfaces can cross each other, creating a CI whenever the conditions $\cos\theta = 0$ ($\theta = \pi/2$) and $V_1(R) = V_2(R) - \hbar\omega_L$ are simultaneously fulfilled.[1,2]

The spatial and the energetic positions of the LICI can be modified by varying the frequency of the laser light. Increasing the frequency, for example, moves the CI to a smaller internuclear distance and to a lower energetic position. The steepness of the CI cone formed by the adiabatic surfaces, which is related to the strength of the nonadiabatic coupling, can be controlled by the laser intensity.

Studying the dissociation dynamics in the LICI framework, we have to solve the time-dependent nuclear Schrödinger equation (TDSE) with the Hamiltonian H described by eq 1. One of the most efficient approaches for this is the MCTDH (multi-configuration time-dependent Hartree) method.[47−51] To characterize the vibrational degree of freedom, we have used FFT-DVR (fast Fourier transformation-discrete variable

dx.doi.org/10.1021/jp504889e | J. Phys. Chem. A XXXX, XXX, XXX−XXX

representation) with N_R basis elements distributed within the range from 0.1 a.u. to 80 a.u. for the internuclear separation. The rotational degree of freedom was described by Legendre polynomials $\{P_J(\cos\ \theta)\}_{j=0,1,2,...,N\theta}$. These so-called primitive basis sets (χ) were used to represent the single particle functions (ϕ), which in turn were used to represent the wave function

$$\phi_{j_q}^{(q)}(q,\ t) = \sum_{l=1}^{N_q} c_{j_q l}^{(q)}(t)\chi_l^{(q)}(q) \qquad q = R,\ \theta \tag{2}$$

$$\psi(R,\ \theta,\ t) = \sum_{j_R=1}^{n_R}\sum_{j_\theta=1}^{n_\theta} A_{j_R,j_\theta}(t)\phi_{j_R}^{(R)}(R,\ t)\phi_{j_\theta}^{(\theta)}(\theta,\ t)$$

In the actual calculations, we have used N_R = 2048 and, depending on the light intensity, N_θ = 6, ..., 70. On both diabatic surfaces and for both degrees of freedom a set of n_R = n_θ = 3, ..., 25, single particle functions were applied to construct the nuclear wave packet of the system. (The actual value of N_θ and n_R = n_θ was chosen depending on the peak field intensity I_0.) All calculations were converged with these parameters. The solution of the MCTDH equations with the ansatz in eq 2 is used to calculate the total dissociation probability, the KER, and the angular distribution of the molecular fragments[49]

$$P_{\text{diss}} = \int_0^\infty \mathrm{d}t\ <\psi(t)|W|\psi(t)> \tag{3}$$

$$P_{\text{ker}}(E) = \int_0^\infty \mathrm{d}t \int_0^\infty \mathrm{d}t' <\psi(t)|W|\psi(t')> \mathrm{e}^{-iE(t-t')} \tag{4}$$

where $-iW$ is the complex absorbing potential (CAP) discussed in ref 48 and employed at the last 5 a.u. of the grid of the vibrational degree of freedom and

$$P(\theta_j) = \frac{1}{w_j}\int_0^\infty \mathrm{d}t <\psi(t)|W_{\theta_j}|\psi(t)> \tag{5}$$

where $-iW_{\theta_j}$ is the projection of the CAP to a specific point of the angular grid (j = 0, ..., N_θ), and w_j is the weight related to this grid point according to the applied DVR.

Throughout the calculations the initial nuclear wave function (at $t \ll 0$ fs) was assumed to be in its rotational ground state (J = 0) and in one of its vibrational eigenstates (ν = 0, 1, 2, 3, 4, 5, 6, 7, 8, 9). Initially, the molecules are thus assumed in the numerical calculations to be nonaligned and isotropically distributed and subject to linearly polarized Gaussian laser pulses centered around t = 0 fs. The wavelengths and the pulse duration in full width at half-maximum (fwhm) are 150−250 nm and t_{pulse} = 30 fs, respectively. The energies of the different vibrational levels as well as the spatial and energetic positions of the LICIs corresponding to the laser wavelength which would make the LICIs coincide with these vibrational levels are collected in Table 1. These wavelengths are called resonant wavelengths. For further information, see Figure 1.

III. RESULTS AND DISCUSSION

The aim of this section is to describe and characterize the photodissociation process of the D_2^+ molecule in a LICI situation where the system is initially in its electronic ground state and the initial nuclear wave packet is chosen to be in its rotational ground state (J = 0) but in one of its vibrational eigenstate (ν = 0, 1, 2, 3, 4, 5, 6, 7, 8, 9). For that purpose, the KER spectra, the total dissociation probabilities, and the angular distributions were calculated. Several different intensity values of the exciting laser pulse have been employed ranging from 3×10^{11} to 1×10^{14} W/cm^2. We note here that the dissociation dynamics starting from the ν = 0, 1, 2, 3, 4 levels has been partially discussed previously,[8] with emphasis on the mechanism of bond softening and bond hardening. Our work addresses all of the previously mentioned levels but mostly focuses on the ν = 5 and higher levels at $\hbar\omega$ = 6.199 eV/λ = 200 nm. These levels provide an unexpected phenomenon that cannot be explained straightforwardly by bond softening and hardening.

Table 1. Energy (E_ν) and Wavelength Values of the Different Vibrational Levels (ν)[a]

ν	E_ν (eV)	R_ν^* (a.u.)	$\hbar\omega_{L,\nu}^*$ (eV)	λ_ν^* (nm)
0	−2.69	2.29	9.54	130.08
1	−2.49	2.55	7.91	156.67
2	−2.30	2.76	6.83	181.47
3	−2.11	2.94	5.98	207.35
4	−1.94	3.12	5.27	235.32
5	−1.77	3.29	4.66	266.34
6	−1.61	3.46	4.11	301.45
7	−1.46	3.64	3.63	341.64
8	−1.31	3.81	3.20	387.73
9	−1.17	3.99	2.81	441.83

[a]Zero of the scale is the energy of $D^+ + D$. In addition, R_ν^* is the internuclear distance where the energy of the ground electronic states ($1s\sigma_g$) is equal to the energy of the given vibrational level ($E_{1s\sigma_g}(R_\nu^*) = E_\nu$); $\hbar\omega_{L,\nu}^*(= E_{2p\sigma_u}(R_\nu^*) - E_{1s\sigma_g}(R_\nu^*))$ is the resonant photon energy where the LICI will coincide with a vibrational level ν; λ_ν^* is the corresponding wavelength.

A. Kinetic Energy Release and Total Dissociation Probability. The results for the KER spectra (eq 4) are collected in Figure 2. For the simulations, an initially unaligned (isotropic) distribution of the molecules was assumed. Several different laser intensities were applied ranging from 3×10^{11} to 1×10^{14} W/cm^2. Striking at first sight is that for lower intensities the value of the dissociation probability from the vibrational eigenstate ν = 5 is very small (practically zero). This trend is slowly changing toward higher intensities. From ~10^{13} W/cm^2, the flux starts to grow, but its value still remains moderate even at the largest studied intensity (1×10^{14} W/cm^2). To explain this phenomenon, we recall here our previous works,[3,4,7,8] in which detailed explanations were given concerning the role of rotation in the correct dynamical description. It was demonstrated that the inclusion of the rotation as a dynamical variable in the nuclear Hamiltonian implies the formation of a LICI even in diatomic molecules. The LICI then introduces an intense nonadiabatic coupling and strongly mixes the rotational and vibrational motions in both electronic states. These surfaces are the $V_1(R)$ and $V(R) - \hbar\omega_L$ diabatic dressed states. After transforming the diabatic Hamiltonian (Figure 1) to the adiabatic picture, we obtain the light-induced adiabatic potentials V_{lower} and V_{upper} (Figure 1). It is known that the strengths of the nonadiabatic coupling are determined by the intensity of the light; therefore, to some extent the shape of the adiabatic PES is also related to the intensity. The different intensities provide slightly different adiabatic surfaces and adiabatic energy levels. In Figure 3A,B, we displayed two different adiabatic potential energy curves together with the adiabatic energy levels for the case of two different intensities (3×10^{13} and 1×10^{12} W/cm^2). We also

dx.doi.org/10.1021/jp504889e | J. Phys. Chem. A XXXX, XXX, XXX−XXX

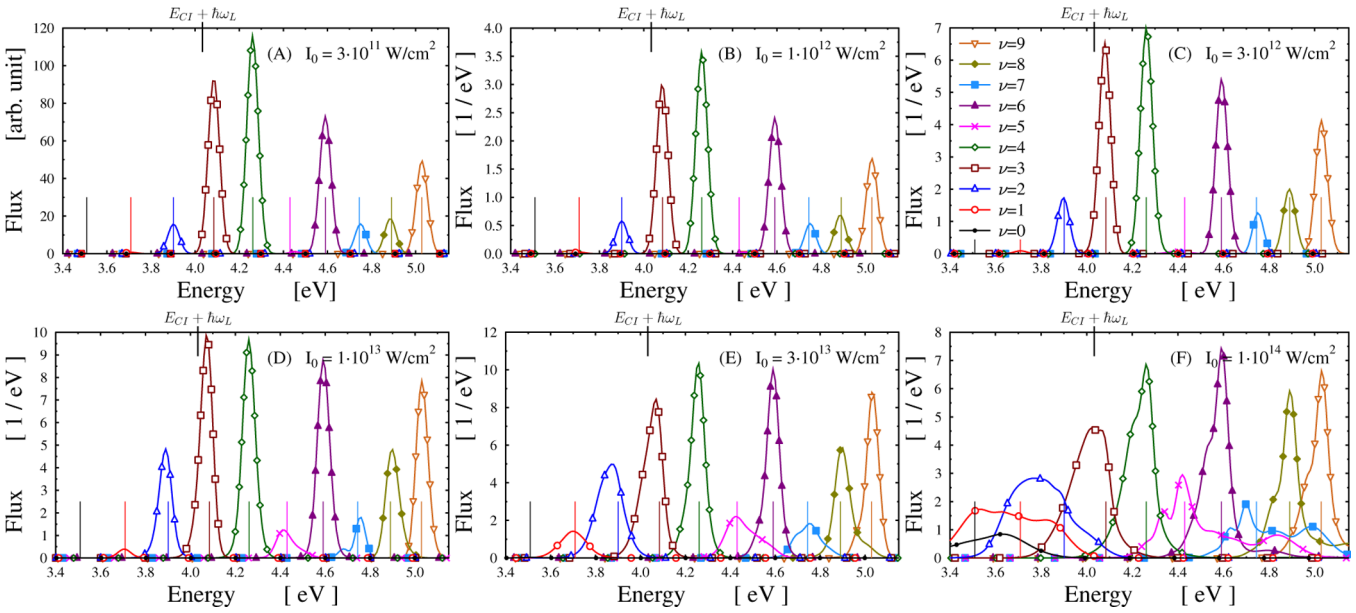

Figure 2. Kinetic energy release (KER) spectra of the D_2^+ photofragments for isotropic initial orientation from 3×10^{11} to 1×10^{14} W/cm^2 intensities. All figures are obtained from the 2D model assuming LICI situation. Vertical lines denote the different vibrational levels of the D_2^+ molecule in the field free case shifted by the photon energy ($\hbar\omega_L$ = 6.199 eV).

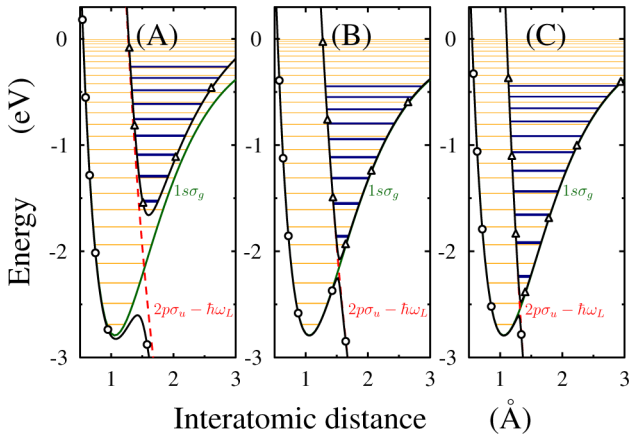

Figure 3. Diabatic and adiabatic cuts of the potential energy surfaces along the interatomic separation at θ = 0. Diabatic energies of the ground ($1s\sigma_g$; solid green) and the field-dressed excited ($2p\sigma_u - \hbar\omega_L$; dashed red line) states are displayed. The adiabatic upper and lower curves are denoted by solid black lines. (A) Laser intensity and wavelength are 3×10^{13} W/cm^2 and λ = 200 nm, respectively. (B) Intensity and the wavelength are 1×10^{12} W/cm^2 and λ = 200 nm, respectively. (C) Intensity and the wavelength are 1×10^{12} W/cm^2 and λ = 150 nm, respectively. The different horizontal lines provide the appropriate adiabatic (in black) and diabatic (in orange) vibrational energy levels.

presented the diabatic potential energy together with its vibrational energy levels. Because of the finite time of the laser pulse, the adiabatic electronic states have a finite lifetime as well. Under very special circumstances, when one of the eigenvalues of the upper adiabatic potential coincides with the energy level of a certain vibrational eigenstate on the diabatic surface, the nuclear wave packet that started from this particular vibrational eigenstate spends a non-negligible amount of time in the upper adiabatic potential before reaching the asymptotic region. The system somehow is being trapped for a while in the upper adiabatic potential. This might be the reason that the dissociation probability from this vibrational eigenstate is hardly measurable. When the intensity slowly changes so does the shape of the adiabatic PES, and the adiabatic energy levels shift accordingly. (See Figure 3A,B.) The value of the shifted adiabatic level and that of the vibrational diabatic level corresponding to the initial energy of the nuclear wave packet (the latter, of course remains unchanged as the intensity changes) no longer match; therefore, some parts of the wave packet do reach the asymptotic region, providing non-negligible flux to the spectrum of this particular vibrational state. The proportion of the vibrational wave packet that reaches the asymptotic region relatively quickly, is strongly dependent on how much the intensity has been changed. The more the initial energy of the vibrational wave packet and that of the particular energy level of the adiabatic potential differ from each other, the more particles will dissociate and reach the region. This dynamical process is illustrated by the KER shown in the panels of Figure 2.

So far we have not varied the frequency of the laser pulse in the calculations. A laser pulse with the frequency ω_L = 6.199 eV (λ = 200 nm) was applied. As previously discussed, the positions of the LICIs are determined by the laser frequency. When increasing the frequency, the position of the LICI is moving to the left in Figure 1, and the opposite is true in the reverse case. This implies that the values of the energy levels of the adiabatic potential also depend on the frequency of the applied laser field. Correspondingly, the shapes of the adiabatic PESs belonging to two different (ω_L = 6.199 eV, λ = 200 nm and ω_L = 8.266 eV, λ = 150 nm) photon energies also change. (See Figure 3B,C.) For illustration, we also displayed in these panels the two diabatic potentials cuts with the corresponding vibrational levels.

To carry out a more detailed analysis, we have performed in addition 1D calculations by keeping θ = 0. By choosing a particular energy/wavelength interval of the laser field (ω_L = 8.266 eV, λ = 150 nm and ω_L = 4.959 eV, λ = 250 nm) and varying continuously the wavelengths in this interval while keeping the intensity fixed (1×10^{11} W/cm^2), we were

dx.doi.org/10.1021/jp504889e | J. Phys. Chem. A XXXX, XXX, XXX−XXX

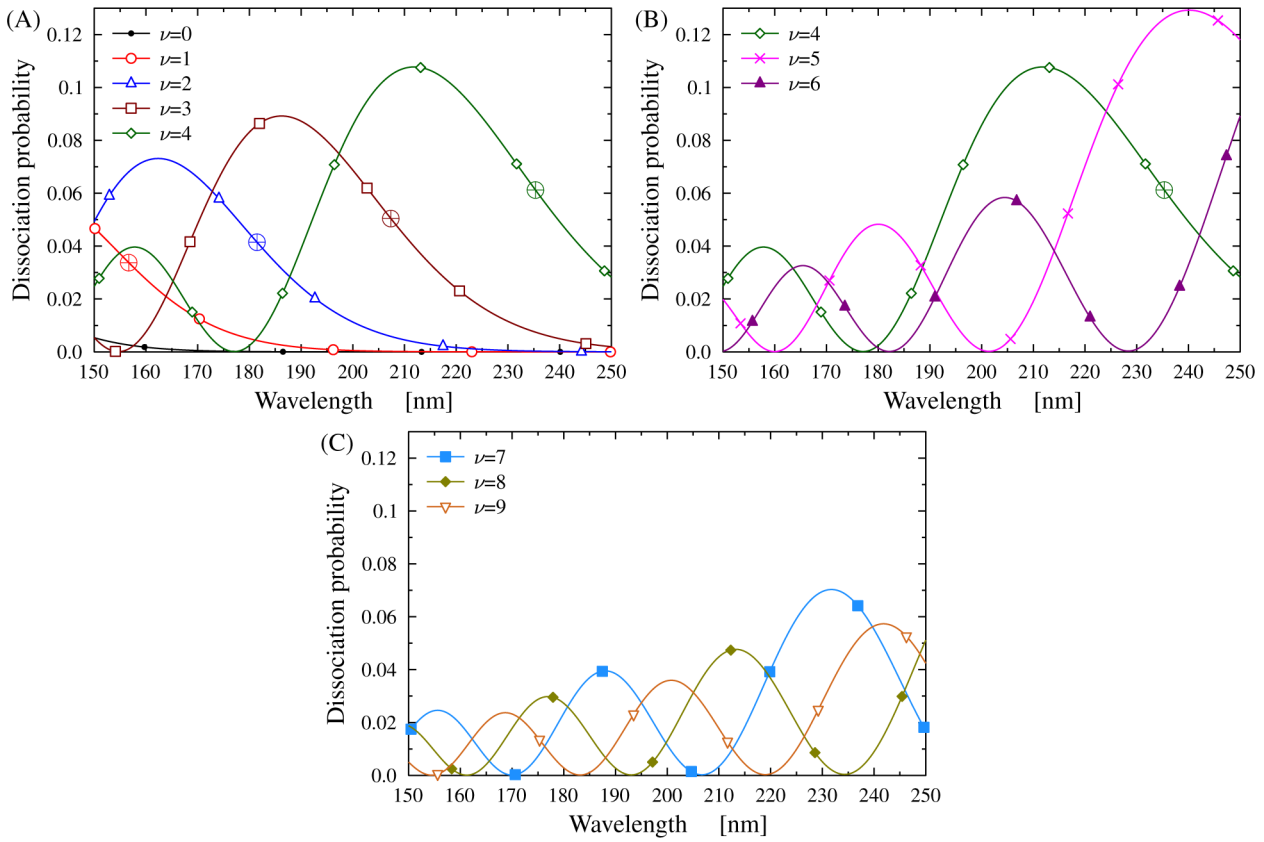

Figure 4. Total dissociation probabilities computed in 1D as a function of laser wavelength for different vibrational eigenstates. Ten different vibrational eigenstates (ν = 0, 1, 2, 3, 4, 5, 6, 7, 8, and 9) are studied. The applied energy/wavelength interval and the intensity are ($\hbar\omega$ = 8.266 eV/λ = 150 nm and $\hbar\omega$ = 4.959 eV/λ = 250 nm) and 1×10^{11} W/cm^2, respectively. (The symbol $\oplus$ denotes the wavelength of λ_ν^*, see Table 1.) The minimum positions of a curve belonging to a particular vibrational quantum number indicate the wavelength values for which the corresponding dissociation probabilities are smallest.

searching for those vibrational eigenstates and wavelength of the photons for which the dissociation probabilities are approximately equal to zero. The pictures demonstrating this search are shown in Figure 4. We observe that several matching pairs of the vibrational quantum numbers and laser wavelengths exist in the studied parameter range, where the dissociation probabilities are close to zero. Numerical results are collected in Table 2. Here the corresponding vibrational quantum numbers and the wavelengths together with the value of the respective dissociation probabilities are collected. By studying Table 2, we find that for large diabatic vibrational quantum numbers more than one minimum position exists in the studied energy interval. This is not surprising because the relative positions of the adiabatic energy levels of the upper adiabatic potential to the energy level of the initial vibrational state at λ = 150 nm determine the possible numbers of minima when we increase the wavelength of the laser field. The higher the initial vibrational state, the larger the number of potentially possible minima. For higher initial states ($\nu > 6$), the lowest lying energy levels of the upper adiabatic potential (ν' = 0, ...) do not provide a minimum in our study as we restrict the value of the wavelength below λ = 250 nm.

To further analyze the results, we present the total dissociation probability P_{diss} of the photofragments (eq 3) as a function of laser intensity (see Table 3) as well but now for fixed laser frequency ω_L = 6.199 eV (λ = 200 nm). From now, we return to the 2D simulations again. Note that for ω_L = 6.199 eV (λ = 200 nm) the ν = 0, 1, 2 vibrational levels are below the

Table 2. Minima of the Dissociation Probabilities for the Different Diabatic Vibrational Levels (ν) as a Function of Laser Wavelength Provided by 1D Calculations[a]

ν	λ (nm)	$P_{diss} \times 10^4$	$\hbar\omega_L$ (eV)	$(E_\nu - E_{CI})$ (eV)	ν'
3	154.7	0.68	8.016	0.392	0
4	177.1	1.19	7.001	0.394	0
5	160.0	0.87	7.751	0.696	1
5	201.4	1.97	6.156	0.386	0
6	182.1	1.45	6.807	0.685	1
6	228.4	3.18	5.429	0.371	0
7	170.0	1.11	7.293	0.931	2
7	206.7	2.33	5.998	0.664	1
8	161.2	0.88	7.690	1.146	3
8	193.0	1.79	6.422	0.904	2
8	234.3	3.67	5.291	0.635	1
9	154.5	0.72	8.027	1.337	4
9	183.2	1.42	6.769	1.115	3
9	219.0	2.81	5.662	0.868	2

[a]The studied energy/wavelength interval is ($\hbar\omega_L$ = 8.266 eV, λ = 150 nm and $\hbar\omega_L$ = 4.959 eV, λ = 250 nm). ν' denotes the vibrational energy levels of the upper adiabatic surface that coincide with the level ν. The applied laser field intensity and pulse length are 10^{11} W/cm^2 and t_{pulse} = 30 fs, respectively.

energy of the LICI (E_{LICI} = −2.1661 eV), and the other vibrational states are above it. (See Figure 1.) At small intensities the flux of the low vibrational levels (ν = 0, 1) is small due to the potential barrier, while from the ν = 3 and 4

dx.doi.org/10.1021/jp504889e | J. Phys. Chem. A XXXX, XXX, XXX−XXX

Table 3. Total Dissociation Probabilities As a Function of the Field Intensities for the Different Vibration Levels[a]

I_0	$\nu = 0$	$\nu = 1$	$\nu = 2$	$\nu = 3$	$\nu = 4$	$\nu = 5$	$\nu = 6$	$\nu = 7$	$\nu = 8$	$\nu = 9$
1×10^{11}	1.9×10^{-6}	1.7×10^{-4}	0.0037	0.0232	0.0291	2.4×10^{-4}	0.0180	0.0038	0.0044	0.0120
3×10^{11}	5.6×10^{-6}	5.1×10^{-4}	0.0113	0.0669	0.0830	6.4×10^{-4}	0.0522	0.0111	0.0133	0.0353
1×10^{12}	1.9×10^{-5}	0.0018	0.0379	0.1948	0.2339	0.0016	0.1570	0.0334	0.0446	0.1095
3×10^{12}	6.6×10^{-5}	0.0060	0.1150	0.4250	0.4715	0.0064	0.3598	0.0763	0.1339	0.2709
1×10^{13}	3.4×10^{-4}	0.0299	0.3612	0.7143	0.7105	0.1298	0.6204	0.1217	0.3739	0.5263
3×10^{13}	0.0042	0.2081	0.7237	0.9009	0.8757	0.3735	0.7807	0.2574	0.5684	0.6693
1×10^{14}	0.3051	0.7873	0.9502	0.9868	0.9794	0.7483	0.9130	0.5354	0.7514	0.7626
3×10^{14}	0.9251	0.9781	0.9962	0.9993	0.9956	0.8793	0.9577	0.7885	0.7626	0.8769

[a]Maximum intensities are given in W/cm^2. The laser frequency is ω_L = 6.199 eV.

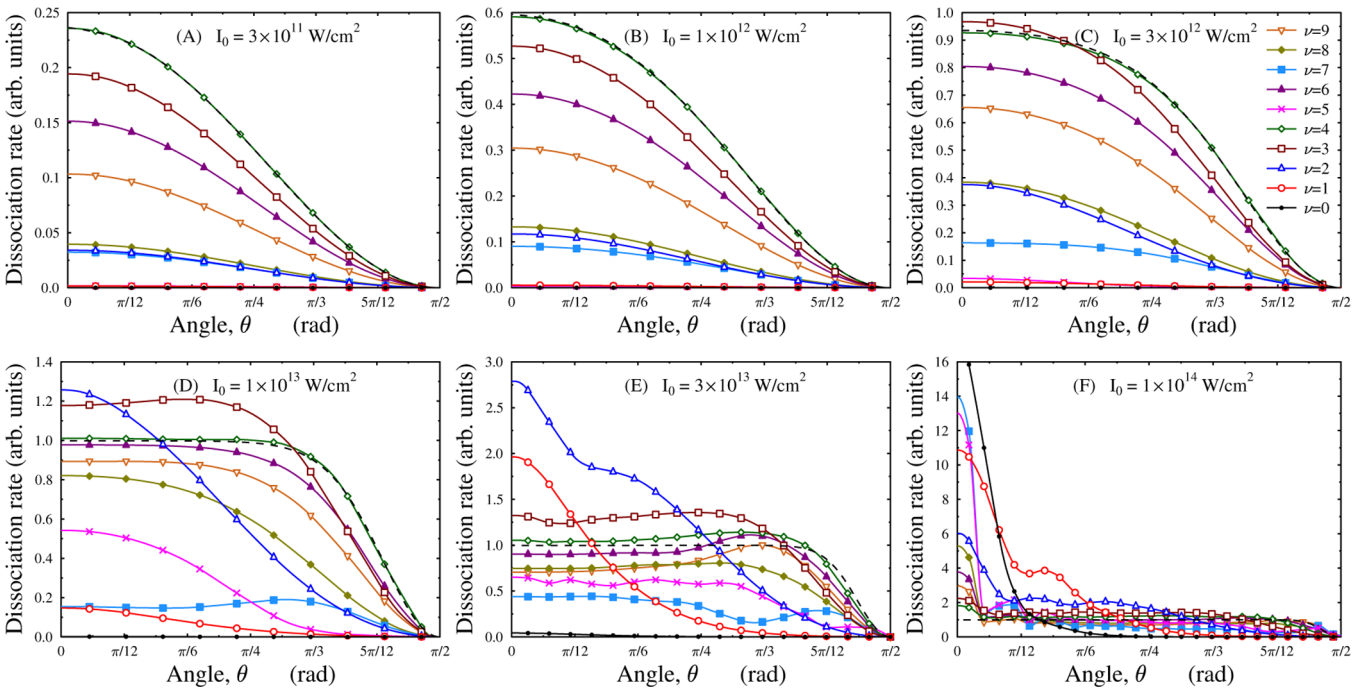

Figure 5. Fragment angular distributions of the dissociating D_2^+ molecule computed in 2D for several different intensities (from 3×10^{11} to 1×10^{14} W/cm^2) and all the studied vibrational states (ν = 0, 1, 2, 3, 4, 5, 6, 7, 8, 9). Dashed lines represent the 1D calculations for ν = 4. No "bumpy" structures appear in 1D.

vibrational levels these numbers are relatively large for those intensity values that are >1×10^{12} W/cm^2. Detailed explanation has already been given for this behavior[8] by using the light-induced potential (LIP) picture. Accordingly, at small or intermediate light intensities the molecules like to follow the diabatic dissociation path, while for large enough intensities they rather tend to follow the adiabatic path. For small light intensities the dissociation behaves linearly with the intensity, whereas at higher intensities up to 10^{14}W/cm^2 this quantity is strongly nonlinear. In the present case, the ν = 0, 1, 2 levels lie in the lower adiabatic potential, but due to the so-called bond softening mechanism they can even dissociate from here for sufficiently large intensities. However, there are states that are in the gap between the two adiabatic potential curves. The number of vibrational states that are in the gap region depends on the value of the intensity. Increasing the intensity, the gap between the two adiabatic potential curves also increases. For those vibrational states that are in the gap region ν = 3, 4, the transition probability is relatively large. Almost all molecules from these states dissociate following the nonadiabatic path, but for the eigenstates that are above the gap region ν = 5, 6, 7, ..., the well-known bond-hardening effect combined with the phenomenon of vibrational trapping previously discussed emerges. The influence of the latter is very strong and almost fully determines the dissociation dynamics from levels ν = 5 or 7, while for the other studied states the previous effect is more pronounced.

B. Angular Distribution. Figure 5 shows the obtained curves for the angular distributions of the photofragments (eq 5). One can see surprising differences between the different panels. The curves are very smooth for (3×10^{11} to 1×10^{13})W/cm^2, but for larger intensities (3×10^{13} to 1×10^{14}) W/cm^2 some distinct modulations emerge on them. The bumpy structure appears in the angular distribution of the photofragments because at large enough intensities the LICI introduces an intense nonadiabatic coupling via mixing the rotational and vibrational motions on both electronic surfaces. By performing the analysis of the nuclear density function,[8] a detailed explanation was given for this effect. It was demonstrated that owing to the strong external electric field rotational nodes are formed, giving rise to the appearance of the quantum interference picture. These quantum interferences are then the sources of the bumpy structure appearing in the angular distribution of the photofragments. Panels E and F

dx.doi.org/10.1021/jp504889e | J. Phys. Chem. A XXXX, XXX, XXX−XXX

display the rich and tangled structure of the angular distribution curves. However, for small and moderate intensity values, the field is not strong enough to build up notable rotational nodes, and therefore interference structure does not appear.

To better visualize of the effect of the LICI, we compared the results obtained from the full 2D calculations with those obtained for a 1D model. In the 1D calculations the rotational degree of freedom was frozen and the LICI thus was not considered. With such conditions, the molecule's initial orientation was not changing during the dissociation process, and the "effective field strength" was the projection of the real field to the axis of the molecule: $\epsilon_0^{\text{eff}} = \epsilon \cos\theta$ ($I_0^{\text{eff}} = I_0 \cdot \cos^2\theta$). In such cases, we have never obtained modulations on the angular distribution curves similar to the ones observed in the full calculations. (The scale on Figure 5 was chosen so that the dissociation rate of 1 represents the total dissociation in a given direction. Larger values in the full calculation mean that some parts of the dissociating particles were rotated by the field to this direction from some different initial ones.) Obtained results clearly demonstrated that the appearance of the bumpy structure on the angular distribution curves is due to the very strong nonadiabatic coupling of the electronic, rotational, and vibrational motions.

IV. CONCLUSIONS

In this work, we have continued our study of the photodissociation dynamics of the D_2^+ molecule in the presence of LICI. The KER spectra, the total dissociation probabilities, and the angular distribution of the photofragments were calculated starting the initial nuclear wave packet before the dissociating pulse arrives from different vibrational eigenstates. The most important yield of this work is that we could explain the unexpected shape of the spectra. The finding that from certain vibrational states the values of the dissociation probabilities are almost zero cannot be interpreted unambiguously by assuming only the bond hardening or vibrational trapping effect. It has been pointed out that the mixed impact of the latter effect combined with the strong nonadiabatic influence provided by the LICI can explain the structure of the spectra correctly.

Among our future prospects is to arrive at a detailed fully quantum dynamical description of the D_2^+ molecule in intense laser field. Among others, we plan to study the simultaneous dissociation and ionization processes within the 2D LICI picture.

AUTHOR INFORMATION

Corresponding Author

*E-mail: vibok@phys.unideb.hu.

Notes

The authors declare no competing financial interest.

ACKNOWLEDGMENTS

We acknowledge the financial support by the Deutsche Forschungsgemeinschaft (Project ID CE10/50-2). A.V. also acknowledges the TÁMOP-4.2.4.A/2-11/1-2012-0001 'National Excellence Program' and the OTKA (NN103251) project.

REFERENCES

(1) Moiseyev, N.; Sindelka, M.; Cederbaum, L. S. Laser-induced Conical Intersection in Molecular Optical Lattices. *J. Phys. B* **2008**, *41*, 221001-1−221001-5.

(2) Sindelka, M.; Moiseyev, N.; Cederbaum, L. S. Strong Impact of Light-induced Conical Intersections on the Spectrum of Diatomic Molecules. *J. Phys. B* **2011**, *44*, 045603-1−045603-6.

(3) Halász, G. J.; Vibók, Á.; Sindelka, M.; Moiseyev, N.; Cederbaum, L. S. Conical Intersections Induced by Light: Berry phase and Wavepacket Dynamics. *J. Phys. B* **2011**, *44*, 175102-1−175102-12.

(4) Halász, G. J.; Sindelka, M.; Moiseyev, N.; Cederbaum, L. S.; Vibók, Á. Light-Induced Conical Intersections: Topological Phase, Wave Packet Dynamics, and Molecular Alignment. *J. Phys. Chem. A* **2012**, *116*, 2636−2643.

(5) Halász, G. J.; Vibók, Á.; Sindelka, M.; Cederbaum, L. S.; Moiseyev, N. The Effect of Light-Induced Conical Intersections on the Alignment of Diatomic Molecules. *Chem. Phys.* **2012**, *399*, 146−150.

(6) Halász, G. J.; Vibók, Á.; Moiseyev, N.; Cederbaum, L. S. Light-Induced Conical Intersections for Short and Long Laser Pulses: Floquet and Rotating Wave Approximations versus Numerical Exact Results. *J. Phys. B* **2012**, *45*, 135101-1−135101-10.

(7) Halász, G. J.; Vibók, Á.; Meyer, H. D.; Cederbaum, L. S. Effect of Light-Induced Conical Intersection on the Photodissociation Dynamics of the D_2^+ Molecule. *J. Phys. Chem. A* **2013**, *117*, 8528−8535.

(8) Halász, G. J.; Vibók, Á.; Moiseyev, N.; Cederbaum, L. S. Nuclear-Wave-Packet Quantum Interference in the Intense Laser Dissociation of the D_2^+ Molecule. *Phys. Rev. A* **2013**, *88*, 043413-1−043413-6.

(9) Cederbaum, L. S.; Chiang, Y. C.; Demekhin, P. V.; Moiseyev, N. Resonant Auger Decay of Molecules in Intense X-Ray Fields: Light-Induced Strong Nonadiabatic Effects. *Phys. Rev. Lett.* **2011**, *106*, 123001-1−123001-4.

(10) Köppel, H.; Domcke, W.; Cederbaum, L. S. Multimode Molecular Dynamics Beyond the Born-Oppenheimer Approximation. *Adv. Chem. Phys.* **1984**, *57*, 59−246.

(11) Yarkony, D. R. Diabolical conical intersection. *Rev. Mod. Phys.* **1996**, *68*, 985.

(12) Baer, M. Introduction to the Theory of Electronic Non-adiabatic Coupling Terms in Molecular System. *Phys. Rep.* **2002**, *358*, 75−142.

(13) Worth, G. A.; Cederbaum, L. S. Beyond Born-Oppenheimer: Molecular Dynamics Through a Conical Intersection. *Annu. Rev. Phys. Chem.* **2004**, *55*, 127−158.

(14) Domcke, W.; Yarkony, D. R.; Köppel, H. *Conical Intersections: Electronic Structure, Dynamics and Spectroscopy*; World Scientific: Singapore, 2004.

(15) Baer, M. *Beyond Born Oppenheimer: Electronic Non-Adiabatic Coupling Terms and Conical Intersections*; Wiley: New York, 2006.

(16) Matsika, S. Conical Intersections in Molecular Systems. *Rev. Comput. Chem.* **2007**, *23*, 83−124.

(17) Kim, J.; Tao, H.; White, J. L.; Petrovic, V. S.; Martinez, T. J.; Bucksbaum, P. H. Control of 1,3-Cyclohexadiene Photoisomerization Using Light-Induced Conical Intersections. *J. Phys. Chem. A* **2012**, *116*, 2758−2763.

(18) Demekhin, P. V.; Cederbaum, L. S. Light-Induced Conical Intersections in Polyatomic Molecules: General Theory, Strategies of Exploitation, and Application. *J. Chem. Phys.* **2013**, *139*, 154314-1−154314-15.

(19) Zavriyev, A.; Bucksbaum, P. H.; Muller, H. G.; Schumacher, D. V. Ionization and Dissociation of H_2 in Intense Laser Fields at 1.064μm, 532 nm, and 355 nm. *Phys. Rev. A* **1990**, *42*, 5500−3513.

(20) Bandrauk, A. D.; Sink, M. Laser Induced Preassociation in the Presence of Natural Predissociation. *Chem. Phys. Lett.* **1978**, *57*, 569−572.

(21) Bandrauk, A. D.; Sink, M. Photodissociation in Intense Laser Fields: Predissociation Analogy. *J. Chem. Phys.* **1981**, *74*, 1110−1117.

(22) Aubanel, E. E.; Gauthier, J. M.; Bandrauk, A. D. Effect of Rotations on Stabilization in High-Intensity Photodissociation of H_2^+. *Phys. Rev. A* **1993**, *48*, 2145−2152.

(23) Charron, E.; Giusti-Suzor, A.; Mies, F. H. Fragment Angular Distribution in one- and two-color Photodissociation by Strong Laser Fields. *Phys. Rev. A* **1994**, *49*, R641−R644.

(24) Chelkowski, S.; Zuo, T.; Atabek, O.; Bandrauk, A. D. Dissociation, Ionization, and Coulomb Explosion of H_2^+ in an Intense

Laser Field by Numerical Integration of the Time-Dependent Schrödinger Equation. *Phys. Rev. A* **1995**, *52*, 2977−2983.
(25) Giusti-Suzor, A.; Mies, F. H.; DiMauro, L. F.; Charron, E.; Yang, B. Dynamics of H_2^+in Intense Laser Fields. *J. Phys. B* **1995**, *28*, 309−339.
(26) Numico, R.; Keller, A.; Atabek, O. Laser-induced Molecular Alignment in Dissociation Dynamics. *Phys. Rev. A* **1995**, *52*, 1298−1309.
(27) Sandig, K.; Figger, H.; Hansch, T. V. Dissociation Dynamics of H_2^+ in Intense Laser Fields: Investigation of Photofragments from Single Vibrational Levels. *Phys. Rev. Lett.* **2000**, *85*, 4876−4879.
(28) Serov, V. N.; Keller, A.; Atabek, O.; Billy, N. Quantitative Theory-Versus-Experiment Comparison of the Intense Laser Dissociation of H_2^+. *Phys. Rev. A* **2003**, *68*, 053401-1−053401-16.
(29) Posthumus, J. H. The Dynamics of Small Molecules in Intense Laser Fields. *Rep. Prog. Phys.* **2004**, *67*, 623−665.
(30) Serov, V. N.; Keller, A.; Atabek, O.; Figger, H.; Pavidic, D. Intense Laser Dissociation of D_2^+: From Experiment to Theory. *Phys. Rev. A* **2005**, *72*, 033413−21.
(31) Uhlmann, M.; Kunert, T.; Schmidt, R. Molecular Alignment of Fragmenting H_2^+ and H_2 in Strong Laser Fields. *Phys. Rev. A* **2005**, *72*, 045402-1−045402−5.
(32) Wang, P. Q.; Sayler, A. M.; Carnes, K. D.; Xia, J. F.; Smith, M. A.; Esry, B. D.; Ben-Itzhak, I. Dissociation of H_2^+ in Intense Femtosecond Laser Fields Studied by Coincidence Three-Dimensional Momentum Imaging. *Phys. Rev. A* **2006**, *74*, 043411-1−043411-21.
(33) Anis, F.; Esry, B. D. Role of Nuclear Rotation in Dissociation of H_2^+ in a Short Laser Pulse. *Phys. Rev. A* **2008**, *77*, 033416-1−033416-11.
(34) Anis, F.; Cackowski, T.; Esry, B. D. Rotational Dynamics of Dissociating H_2^+ in a Short Intense Laser Pulse. *J. Phys. B* **2009**, *42*, 091001-1−091001-6.
(35) Adhikari, S.; Paul, A. K.; Mukhopadhyay, D.; Halász, G. J.; Vibók, Á.; Baer, R.; Baer, M. Molecular Systems in Intense Short-Pulsed External Fields: Application of Space-Time Contours for H_2^+. *J. Phys. Chem. A* **2009**, *113*, 7331−7337.
(36) Paul, A. K.; Adhikari, S.; Baer, M.; Baer, R. H_2^+ Photodissociation by an Intense Pulsed Photonic Fock State. *Phys. Rev. A* **2010**, *81*, 013412-1−013412-10.
(37) Calvert, C. R.; Bryan, W. A.; Newell, W. R.; Williams, I. D. Time-Resolved Studies of Ultrafast Wavepacket Dynamics in Hydrogen Molecules. *Phys. Rep.* **2010**, *491*, 1−28.
(38) Thumm, U.; Niederhausen, T.; Feuerstein, B. Time-Series Analysis of Vibrational Nuclear Wave-Packet Dynamics in D_2^+. *Phys. Rev. A* **2008**, *77*, 063401-1−063401-12.
(39) Fischer, M.; Grossmann, F.; Schmidt, R.; Handt, J.; Krause, S. M.; Rost, J. M. Mixed Quantum-Classical Approach to Multiphoton Dissociation of the Hydrogen Molecular Ion. *New. J. Phys.* **2011**, *13*, 053019-1−053019-14.
(40) Fischer, M.; Lorenz, U.; Schmidt, B.; Schmidt, R. Fragmentation due to Centrifugal Forces in the Photodissociation of H_2^+ in Intense Laser Fields. *Phys. Rev. A* **2011**, *84*, 033422-1−033422-5.
(41) McKenna, J.; Anis, F.; Sayler, A. M.; Gaire, B.; Johnson, N. G.; Parke, E.; Carnes, K. D.; Esry, B. D.; Ben-Itzhak, I. Controlling Strong-Field Fragmentation of H_2^+ by Temporal Effects with Few-Cycle Laser Pulses. *Phys. Rev. A* **2012**, *85*, 023405-1−023405-15.
(42) He, H. X.; Lu, R. F.; Zhang, P. Y.; Han, K. L.; He, G. Z. Dissociation and Ionization Competing Processes for H_2^+ in Intense Laser Field: Which One is Larger? *J. Chem. Phys.* **2012**, *136*, 024311-1−024311-6.
(43) Furukawa, Y.; Nabekawa, Y.; et al. Resolving Vibrational Wave-Packet Dynamics of H_2^+ Using Multicolor Probe Pulses. *Opt. Lett.* **2012**, *37*, 2922−2924.
(44) Handt, J.; Krause, S. M.; Rost, J. M.; Fischer, M.; Grossmann, F.; Schmidt, R. Complete Dynamics of H_2^+ in Strong Laser Fields. *arXiv* **2011**, arXiv:1103.1565v2.
(45) Bunkin, F. V.; Tugov, I. I. Multiphoton Processes in Homopolar Diatomic Molecules. *Phys. Rev. A* **1973**, *8*, 601−612.
(46) Chu, S. I.; Laughlin, C.; Datta, K. Two-Photon Dissociation of Vibrationally Excited H_2^+. Complex Quasi-Vibrational Energy and Inhomogeneous Differential Equation Approaches. *Chem. Phys. Lett.* **1983**, *98*, 476−481.
(47) Meyer, H. D.; Manthe, U.; Cederbaum, L. S. The Multi-Configurational Time-Dependent Hartree Approach. *Chem. Phys. Lett.* **1990**, *165*, 73−78.
(48) Manthe, U.; Meyer, H. D.; Cederbaum, L. S. Wave-Packet Dynamics within the Multiconfiguration Hartree Framework: General Aspects and Application to NOCl. *J. Chem. Phys.* **1992**, *97*, 3199−3213.
(49) Beck, M. H.; Jäckle, A.; Worth, G. A.; Meyer, H. D. The Multiconfiguration Time-Dependent Hartree Method: A Highly Efficient Algorithm for Propagating Wavepackets. *Phys. Rep.* **2000**, *324*, 1−105.
(50) Worth, G. A.; et al. *The MCTDH package*, version 8.2; University of Heidelberg: Heidelberg, Germany, 2000. Meyer, H. D.; et al. *The MCTDH package*, versions 8.3 and 8.4; University of Heidelberg, Germany, 2002 and 2007. http://mctdh.uni-hd.de/.
(51) Meyer, H. D.; Gatti, F.; Worth, G. A. *Multidimensional Quantum Dynamics: MCTDH Theory and Applications*; Wiley-VCH; Weinheim, Germany, 2009.